

Journal of Chemometrics, Vol. 28, 2014, 287-292.

(wileyonlinelibrary.com/journal/cem) DOI: 10.1002/cem.2601

Copyright © 2014 John Wiley & Sons, Ltd.

Classification and unscrambling a class-inside-class situation by object target rotation:

Hungarian silver coins of the Árpád Dynasty, 997 – 1301 AD

Olav H. J. Christie¹, Anita Rácz^{2,4,*}, János Elek³, Károly Héberger⁴

¹ Information Strategies, Stavanger, Norway. E-mail: olav.christie@infostrat.no

² Corvinus University of Budapest, H-1118 Budapest XI., Villányi út 29-43.

E-mail: anita.racz@uni-corvinus.hu

³ Science Port Ltd., H-4032 Debrecen, Egyetem tér 1., E-mail: elek@scienceport.hu

⁴ Research Centre for Natural Sciences, Hungarian Academy of Sciences, H-1117

Budapest XI, Magyar Tudósok krt. 2. E-mail: heberger.karoly@ttk.mta.hu

To whom correspondence should be sent:

Tel.: +36 1 438 11 03; fax: +36 1 438 11 43.

E-mail address: anita.racz@uni-corvinus.hu (A. Rácz).

Abstract

Classification is an important part of chemometrics and mostly based on optimization by vector rotations. The present study is a continuation of the classification of medieval Hungarian silver coins including the 16 kings of the Hungarian Árpád Dynasty (997AD – 1301AD) (Rácz *et al.*: *Heritage Science* 2013 1:2) The Rácz *et al.* paper identified three historical periods of the Árpád Dynasty from chemical data. The aim of the present study is to test whether the classification could be further refined by marker object projection aided classification. It offers an example of the efficiency of this method in unscrambling a class-inside-class situation.

The frequency distribution of concentrations of the coins are skewed and to a certain extent bi-modal, and the arithmetic mean value and standard deviation around the mean frequently used in parametric methods may be poor descriptors of the information carried by the data. We test a combination of principal components decomposition and the non-parametric, non-iterative object target rotation method to overcome some of the theoretical limitations of parametric methods. This test includes identification of archetypical class “Ambassadors” of each of the three historical periods of the Árpád Dynasty and shows a class-inside-class situation.

Keywords: classification, target rotation, X-ray fluorescence spectroscopy, coins, class-inside-class

Introduction

Historical framework

The reign of the Árpád Dynasty coincides with the medieval warm climatic period and ended before the great plague in the 1340ies. In the early Árpád Dynasty period Hungary became a major state with a modernized sociopolitical system divided into three levels, the royal family, the major landowners accredited to nobility by the king, and the farmers living on the remaining land owned by the king.

The mild climate led to expansion of farmland, increased agricultural production and population growth. The need for payment valuables became evident, and the medieval mining industry was ready to deliver substantial amounts of silver.

The present study is a continuation of the classification of medieval Hungarian silver coins including the 16 kings of the Hungarian Árpád Dynasty (997 AD – 1301 AD) [1]. Three historical periods of the Árpád Dynasty have been defined earlier.

Energy dispersive X-ray fluorescence spectroscopy

The heterogeneity of the silver coin alloys in the period of the Árpád Dynasty makes it difficult to establish a reliable method for assigning coins to each single king based on simple statistics of the chemical composition. The energy dispersive X-ray fluorescence spectroscopy (XRF) [2,3] is a non-destructive, fast and reliable analysis of the samples commonly used for studies of the composition of archeological coins.

Earlier studies

Linke *et al.* examined two types of medieval coins with XRF, proton-induced X-ray emission analysis (PIXE) and scanning electron microscopy (SEM/EDX) [4]. The two types of coins were grouped successfully by principal component analysis (PCA), and they also recognized

the unknown coins. Pitarch *et al.* made similar studies of silver coins from the eras of the Spanish War of Independence and of Ancient Greece. [5,6]. Kallithrakas-Kontos *et al.* and Bugoi *et al.* classified ancient coins from the fourth to the first century B.C. by their places of origin and recovery also used PCA [7,8]. Minemasa *et al.* used XRF spectroscopy, PCA and cluster analysis for detection of counterfeit 500¥ coins [9]. The discrimination of valid and counterfeit coins was successful, and they recognized two separate counterfeit groups. Hida *et al.* made a similar study [10]. Rodrigues *et al.* examined 416 silver-copper coins from the Ottoman Empire using several techniques including XRF spectroscopy. They classified the coins by their provenance of origin and observed connection between minor and trace elements and the mints. Again, PCA was used for the evaluation of the data [11]. Reale *et al.* used XRF spectroscopy for studying the correlation between soil characteristics and corrosion products of ancient Italian coins [12].

Methodology

The elemental composition data determined applying X-ray fluorescence spectroscopy were used to analyze silver coins from the Hungarian Árpád Dynasty (997AD – 1301AD) including 16 kings [1]. The coins were classified according to their historical periods. Correct classifications of 76–78% were obtained by PCA, partial least squares discriminant analysis and other statistical analyses of the XRF data.

The first aim of the present study is to select one representative object for the three sections of the Árpád Dynasty (ARP1-ARP3). These objects are called Ambassadors. They were appointed by aid of individual object target rotation to each coin. First, every coin was iteratively subject to target rotation that forms its specific target vector in the variable space. Score values of all other coins in the class are obtained by projection down to that target

vector. This means that there will be one set of object score values for each coin specific target vector. The second aim is to establish the Ambassador's niche in terms of span of score values of the other coins to be accepted as class members.

Marker object projection is a relatively rarely used method for classification, but as a non-parametric technique it is useful for verifying and refining results obtained by other methods [13-19]. The basic idea is illustrated in Figure 1 that refers to a data set with an unspecified number of objects and two variables, y_1 and y_2 . This diagram displays two objects \underline{x}_{k1} and \underline{x}_{k2} , is similar to Figure 1 in Kvalheim [13]. It shows how the projection leads to a score value t_k that indicates the degree of similarity to the marker-object \underline{w}_a .

Figure 1

The Ambassador for each of the three Árpád periods was selected stepwise.

1. Make a separate set of standardized raw data for each of the three Árpád periods.

For the data set of each period:

2. Select a coin in the period as a marker-object (a) and make a marker-object projection of each of the other coins in the period to find the projection score value t_1 . Repeat until all the coins of the period have been selected marker-object:

$$t_l = \underline{x}_l' \underline{x}_k / \|\underline{x}_k\| \quad l = 1, 2, \dots, N \quad (1)$$

3. Calculate the average and the standard deviation for each of the marker-object projection score sets separately and select the marker-object with the lowest standard deviation as the Ambassador marker-object.

The complete set of the three Árpád period coins were projected on to the Ambassador vector of each Árpád period to characterize their similarity to the actual period. We set a strict condition for acceptance of affiliation to the given Árpád period and stated Ambassador coin

score value plus/minus 1.2 times the standard deviation as the upper and lower bond for admission. (The outcome of this classification can be seen later in Table 4.)

Results and discussion

The Árpád Dynasty collection comprises 192 coins. Several of the variables (Ni, Sb, Sn, Ti, and Zn) are absent in more than 60 per cent of the coins and therefore, they were excluded from the present data analysis. The raw data were pre-processed by standardization (mean centered and divided by standard deviation).

The first principal component score values indicate three different periods during the Árpád Dynasty [1] (Figure 2 and Table 1). They correspond to the periods of the I_T system except for minor shifts in the start and finish of the periods.

Figure 2

Figure 3a) and b) are zoomed parts of Fig. 2 and illustrate a shift in score values during the Kálmán (Könyves) period and another one during the reign of András II, one hundred years later. Table 1 shows the earlier published three historical sections in the I_T notation and the sections in ARP notation. The classification systems are almost identical.

Table 1

The ARP notation is based on the score values of the first principal component (Figure 2, 3a and 3b) that can be taken as a monitor of historical periods of the Árpád Dynasty.

Figure 3a and 3b

Basically the ratio between noble metal and copper defines the real value of a coinage but the mercantile belief in the value is decisive. The sudden change in the Hungarian coin metal composition during the reign of Kálmán (Könyves) is possibly an example of coin debasement without subsequent inflation, meaning that, independently of the actual silver

content of the coins, the merchants and lay-man's belief in the value of the coin remained. The debasement seems to have been a pragmatic solution to imminent need of more coins to pay workers and soldiers in a country of material, military, and cultural progress. The situation is exemplified by the fact that king Béla III (1172 – 1196) spent an equivalent of 23 tons of pure silver over 20 years – twice as much as the receipts of the English Crown. Still, we know from among the five Béla III coins in the present collection four of them contain between thirty and forty per cent copper, the remaining one 94 per cent. Fifty-eight of the 77 coins of the ARP2 period have less than 80 per cent silver. Access to silver metal on the open market could possibly have contributed to the shift from the middle to the last part of the Árpád Dynasty when silver from the recently opened Freiberg mines became available.

Table 2 shows that the span of concentrations is very different among the variables, and that the frequency distributions are considerably skewed. This makes the data unfit for standard parametric statistical methods – at least in theory.

Table 2

To make the distributions comparable, the concentration of the coins were sorted among ten concentration compartments for each of the five constituents (Table 3 and Figure 4).

Table 3

Figure 4

Figure 4 illustrates the distributions of the selected constituents. The frequency distributions of Ag and Cu are bi-modal, which strengthens the need for non-parametric methods.

The distributions are typical of numerically closed systems: the coins have five important constituents the concentration of which are summed up to about one hundred – depending on amount of elements present in the original raw data but excluded in the present study for reasons given above. The major constituent would normally be Ag and a smaller

amount of Cu. Furthermore, in the 12th century the Árpád Dynasty kings often debased their coins by replacing substantial amounts of Ag by Cu. This amplifies the negative correlation between Ag and the other constituents.

Under condition that each mintage was done from a homogeneous alloy there are compositional differences between each monetary issue of each king in the Árpád Dynasty. The technology at that time may explain this. Galena (Bleiglanz, PbS) was the major source and may contain substantial amounts of silver metal that was separated from lead in the cupellation process, which oxidizes the lead being deposited at oven walls and thus leaving a melt of pure silver. By late medieval standards the metallurgy in the earliest part of the Árpád Dynasty was primitive and the smelters lacked the skills to produce high-purity silver. In preparation of the minting alloy a small amount of lead was added to improve the hardness of the coins, and various amounts of copper were added for the same reasons or for debasement of the coinage. Occasional amounts of tin, zinc and bismuth may be the outcome either of poor technology or of earlier impure coins added to the melt.

Figure 5 illustrates the extension of debasement in the three periods of the Árpád Dynasty: the vast majority of coins in the ARP1 and ARP3 period hold at least eighty per cent silver. This is in contrast with the coins of the ARP2 period.

Figure 5

As a first step of the object target rotation, the Ambassadors were selected with the least sum of variance criterion in each period. Figure 6 shows the selection in the first period.

Figure 6

The bar length indicates the variance of all the class members to the target object. The small bar of the coin A12d indicates that it is the most central object in the ARP1 class, and consequently being the ARP1 Ambassador. The outcome of the classification based on the ARP1, ARP2, and ARP3 Ambassadors, respectively, are given in Table 4

Table 4

There is only one coin from the István III period (marked by an asterix).

Figure 7a-c)

Figure 7 was made for a better understanding and visualization of the interrelations between the Ambassador niches: it is a Venn diagram type representation known from set theory. The ellipses qualitatively reflect the fractions of the coins for each king included in the niche. The areas are roughly corresponding to the fractions of Table 4. The classification by non-iterative object target rotation is an inspection of the multidimensional variable space as seen from the center of one object vector and the perspective depends on the location of this center. Therefore, depending on the viewpoint, different class interrelations can be seen.

The ARP 1 niche includes none of the ARP 2 coins and some of the ARP 3 ones (Fig. 7a). The ARP 2 niche includes none of the ARP 1 coins and a majority of the ARP 3 coins (Fig. 7b), and the ARP 3 niche includes all but one of the ARP 1 coins and some of the ARP 2 coins (Fig. 7c).

Conclusion

The nonparametric marker object projection method can extract information, which is not accessible using classical chemometric tools; that is, it can be an alternative to unsupervised and supervised pattern recognition methods such as PCA and partial least squares discriminant analysis, respectively. The object target rotation is especially useful if the distributions are skewed and/or bimodal.

The triumph of the methodology is the efficiency of class assignment combined with the ability to resolve the class-inside-class situation.

References

1. RÁCZ A, Héberger K, Rajkó R, Elek J. Classification of Hungarian medieval silver coins using X-ray fluorescent spectroscopy and multivariate data analysis. *Heritage Science* 2013; **1**: 2.
2. Beckhoff B, Kanngießer B, Langhoff N, Wedell R, Wolff H *Handbook of Practical X-ray Fluorescence Analysis*. Springer: Berlin, 2006.
3. Cesareo R. *X-Ray Fluorescence Spectrometry*. Ullmann's Encyclopedia of Industrial Chemistry, Wiley: New York, 2010.
4. Linke R, Schreiner M, Demortier G. The application of photon, electron and proton induced X-ray analysis for the identification and characterisation of medieval silver coins. *Nuclear Instruments and Methods in Physics Research B* 2004; **226**: 172–178.
5. Pitarch A, Queralt I, Alvarez-Perez A. Analysis of Catalanian silver coins from the Spanish War of Independence period (1808–1814) by Energy Dispersive X-ray Fluorescence. *Nuclear Instruments and Methods in Physics Research B* 2011; **269**: 308–312.
6. Pitarch A, Queralt I. Energy dispersive X-ray fluorescence analysis of ancient coins: The case of Greek silver drachmae from the Emporion site in Spain. *Nuclear Instruments and Methods in Physics Research B* 2010; **268**: 1682–1685.
7. Kallithrakas-Kontos N, Katsanos AA, Touratsoglou J. Trace element analysis of Alexander the Great's silver tetradrachms minted in Macedonia. *Nuclear Instruments and Methods in Physics Research B* 2000; **171**: 342–349.
8. Bugoi R, Constantinescu B, Constantin F, Catana D, Plostinaru D, Sasianu A. Archaeometrical studies of Greek and Roman silver coins. *Journal of Radioanalytical and Nuclear Chemistry* 1999; **242**: 777–781.

9. Hida M, Sato H, Sugawara H, Mitsui T. Classification of counterfeit coins using multivariate analysis with X-ray diffraction and X-ray fluorescence methods. *Forensic Science International* 2001; **115**: 129-134.
10. Hida M, Mitsui T. Application of multivariate analysis to forensic science samples. *Bunseki Kagaku* 1998; **47**: 645-651.
11. Rodrigues M, Schreiner M, Mäder M, Melcher M, Guerra M, Salomon J, Radtke M, Alram M, Schindel N. The hoard of Beçin—non-destructive analysis of the silver coins. *Applied Physics A: Materials Science & Processing* 2010; **99**: 351-356.
12. Reale R, Plattner SH, Guida G, Sammartino MP, Visco G. Ancient coins: cluster analysis applied to find a correlation between corrosion process and burial soil characteristics. *Chemistry Central Journal* 2012; **6**: 2.
13. Kvalheim OM. Latent-Structure Decompositions (Projections) of Multivariate Data. *Chemometrics and Intelligent Laboratory Systems* 1987; **2**: 283-290.
14. Kvalheim OM, Karstang TV. Interpretation of Latent-Variable Regression Models. *Chemometrics and Intelligent Laboratory Systems* 1989; **7**: 39-51.
15. Hove H, Liang YZ, Kvalheim OM. Trimmed object projections: a nonparametric robust latent structure decomposition method. *Chemometrics and Intelligent Laboratory Systems* 1995; **27**: 33-40.
16. Christie OHJ. Data laundering leading to meaningful principal component classification criterion and map attribute in surface geochemistry. *Aquatic Sciences* 1995; **57**: 242-254.
17. Christie OHJ. The influence of skewed measurement distribution commonly found in analytical geochemistry. *Analytical Letters* 1979; **12**: 979 – 993.

- 18 Christy AA, Kvalheim OM, Libnau FO, Aksnes G, Toft J. Interpretation of chemical structural changes by target-projection analysis of infrared profiles. *Vibrational Spectroscopy* 1993; **6**: 1-14.
19. Kvalheim OM, Chan HY, Benzie IFF, SzetoYT, Tzang AHC, Mok DKW, Chau FT. Chromatographic profiling and multivariate analysis for screening and quantifying the contributions from individual components to the bioactive signature in natural products. *Chemometrics and Intelligent Laboratory Systems* 2011; **107**: 98–105.

Table 1

Kings of the Árpád Dynasty and notations.

Árpád Dynasty		Present paper notation		I_T
997-1038	Saint István I (crowned in 1000)	A11	ARP1	1
1074-1077	Géza I	A12		
1077-1095	Saint László I	A13		
1095-1116	Kálmán (Könyves)	A14		
1116-1131	István II	A21	ARP2	2
1131-1141	Béla II	A22		
1141-1162	Géza II	A23		
1162-1172	István III	A24		
1162-1163	László II	A25		
1172-1196	Béla III	A26		
1196-1204	Imre I	A27		
1205-1235	András II	A31	ARP3	3
1235-1270	Béla IV	A32		
1270-1272	István V	A33		
1272-1290	László IV	A34		
1290-1301	András III	A35		

Table 2

Concentration spans and distribution skewness of the Árpád Dynasty coins.

	Ag	Cu	Pb	Fe	Bi
Min	0.00	0.00	0.00	0.00	0.00
Max	98.50	92.71	12.18	1.99	0.63
Skewness	-1.85	1.77	4.32	3.16	1.62

Table 3

Number of coins in each compositional compartment

Compartment	Ag	Cu	Pb	Bi	Fe
C1 lowest conc.	3.00	37.00	63.00	26.00	22.00
C2	2.00	21.00	23.00	43.00	14.00
C3	3.00	10.00	7.00	22.00	3.00
C4	3.00	11.00	0.00	9.00	4.00
C5	4.00	6.00	1.00	1.00	0.00
C6	13.00	1.00	2.00	2.00	3.00
C7	7.00	3.00	0.00	0.00	1.00
C8	22.00	4.00	0.00	1.00	1.00
C9	35.00	4.00	0.00	1.00	1.00
C10 highest conc.	90.00	9.00	1.00	1.00	1.00

Table 4

Assignment of the coins to the ARP1, ARP2, and ARP3 niches, respectively. Membership indicates how large fraction of the coins of each king is included in the niche.

Assignment to the ARP1 niche			Assignment to the ARP2 niche			Assignment to the ARP3 niche		
King	Member-ship	Niche	King	Member-ship	Niche	King	Member-ship	Niche
Saint István I	100 %		Saint István I	0 %		Saint István I	100 %	
Géza I	100 %	ARP1	Géza I	0 %	ARP1	Géza I	100 %	ARP1
Saint László I	89 %		Saint László I	0 %		Saint László I	89 %	
Kálmán (Könyves)	8 %	_____	Kálmán (Könyves)	33 %	_____	Kálmán (Könyves)	33 %	_____
István II	0 %		István II	86 %		István II	29 %	
Béla II	0 %		Béla II	81 %		Béla II	7 %	
Géza II	0 %		Géza II	100 %		Géza II	0 %	
István III	0 %	ARP2	István III	100 %	ARP2	István III	0 %	ARP2
László II	0 %		László II	67 %		László II	33 %	
Béla III	0 %		Béla III	100 %		Béla III	0 %	
Imre I	0 %		Imre I	90 %		Imre I	0 %	
András II	16 %	_____	András II	63 %	_____	András II	37 %	_____
Béla IV	24 %		Béla IV	76 %		Béla IV	41 %	
István V	8 %	ARP3	István V	92 %	ARP3	István V	50 %	ARP3
László IV	40 %		László IV	80 %		László IV	67 %	
András III	10 %		András III	70 %		András III	50 %	

Caption to figures

Figure 1

Projection of two objects, \underline{x}_{k1} (left) and \underline{x}_{k2} (right) on a marker-object vector, \underline{w}_a (further on Ambassador), to produce marker-object (a) projection score values, \underline{t}_{k1a} (left) and \underline{t}_{k2a} (right) illustrated in a diagram of two perpendicular axes, y_1 and y_2 , representing unit vectors, \underline{e}_1 and \underline{e}_2 , of two variables. The object \underline{x}_{k1} to the left has a higher score than the object \underline{x}_{k2} to the right, meaning that \underline{x}_{k1} is more similar to the marker-object than is the \underline{x}_{k2} object.

Figure 2

The first principal component of the Árpád Dynasty coins reflects the balance between silver and copper in the minting alloys.

Figure 3a) and b)

These figures are zoomed parts of Fig. 2 showing the transitions between the Árpád Dynasty coin history periods.

Figure 4

Frequency distributions divided in ten compositional compartments based on data from Table 3.

Figure 5

Number of coins from the three periods of the Árpád Dynasty containing more or less than 80 per cent silver.

Figure 6

Least sum of variances criterion for selection of the Ambassador for the ARP 1 class

Figure 7a-c)

Visualization of the class interrelationships as seen from each Ambassador location in the multidimensional variable space.

Figure 1.

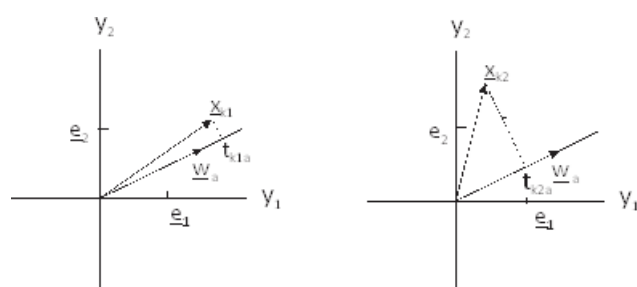


Figure 2.

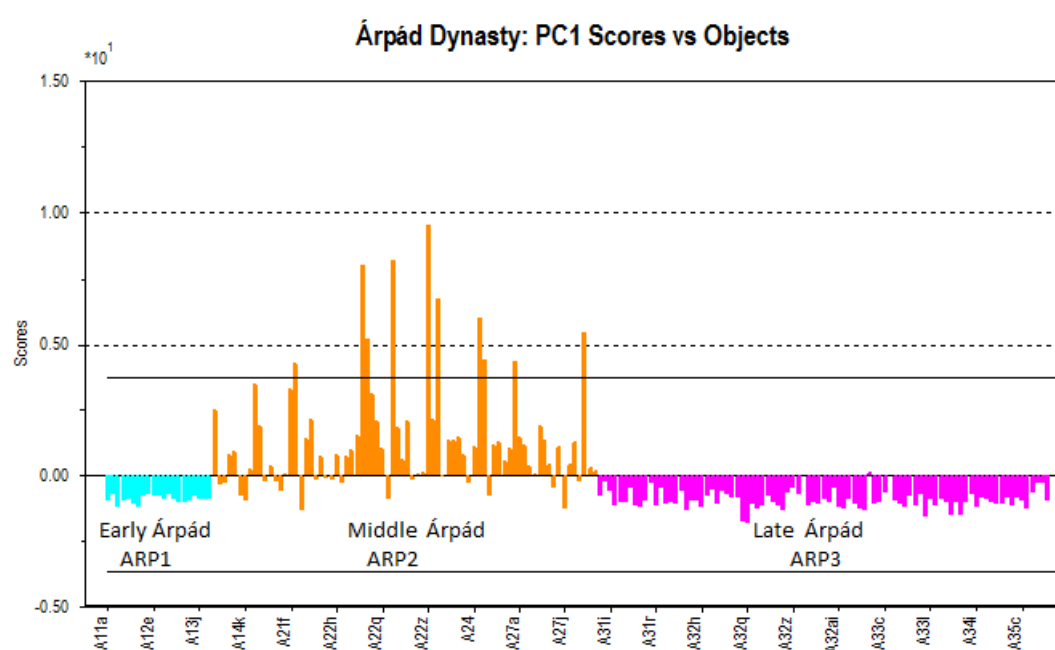


Figure 3a.

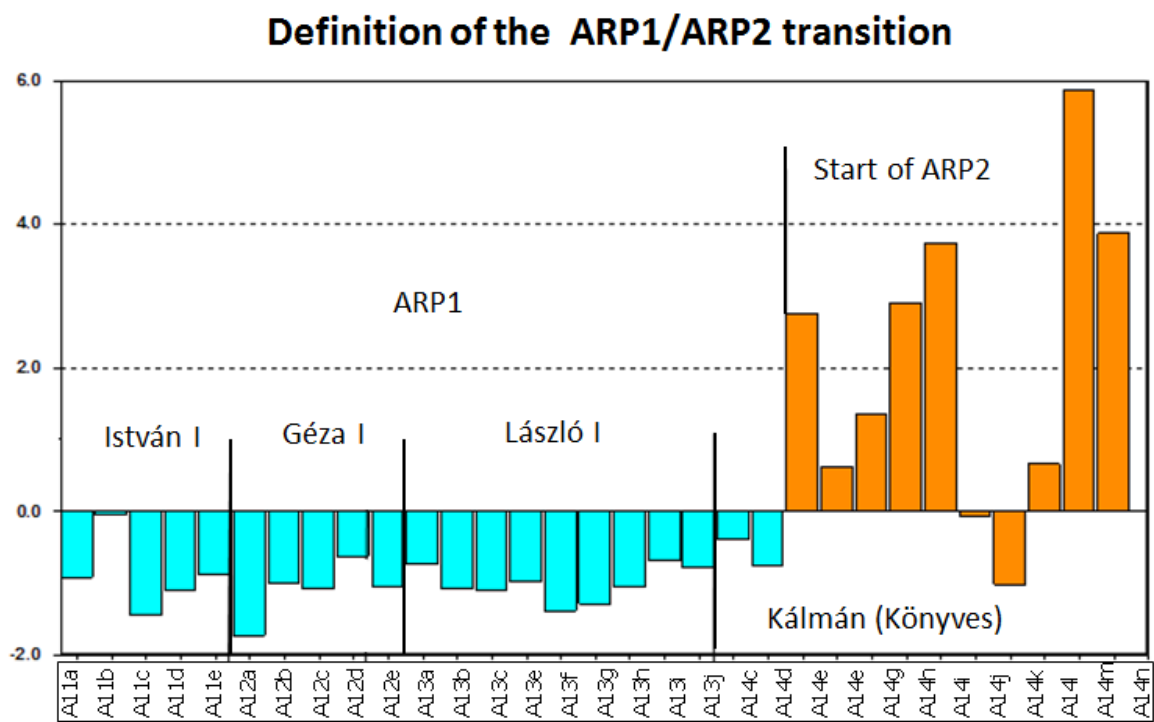


Figure 3b.

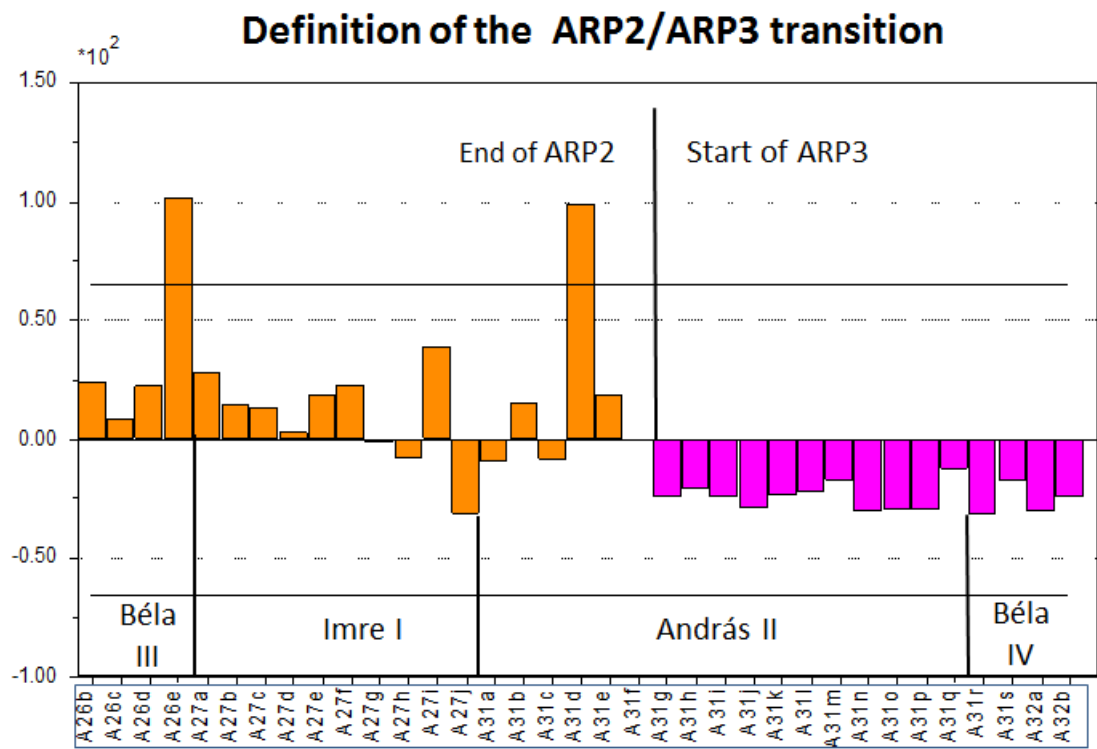


Figure 4.

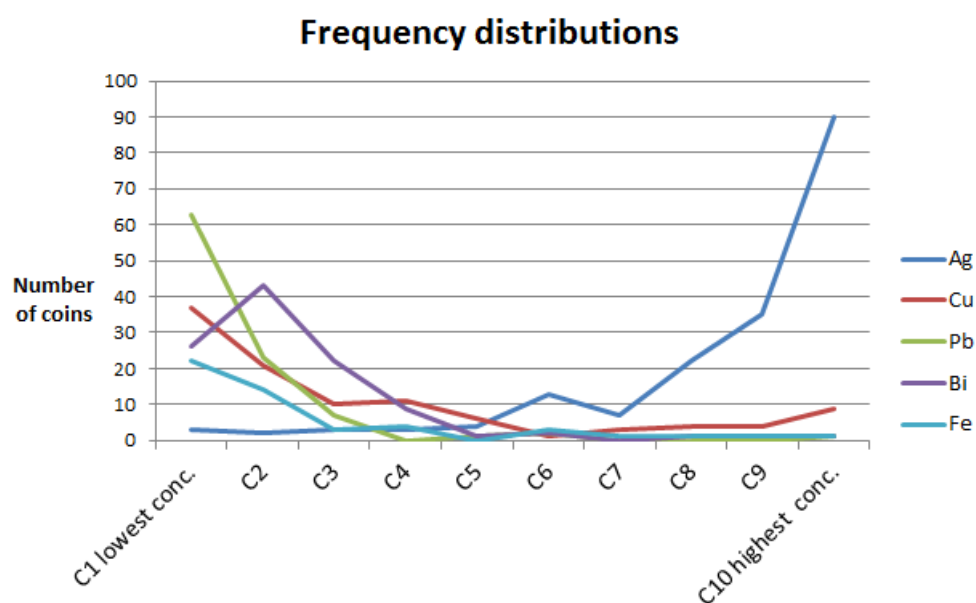


Figure 5.

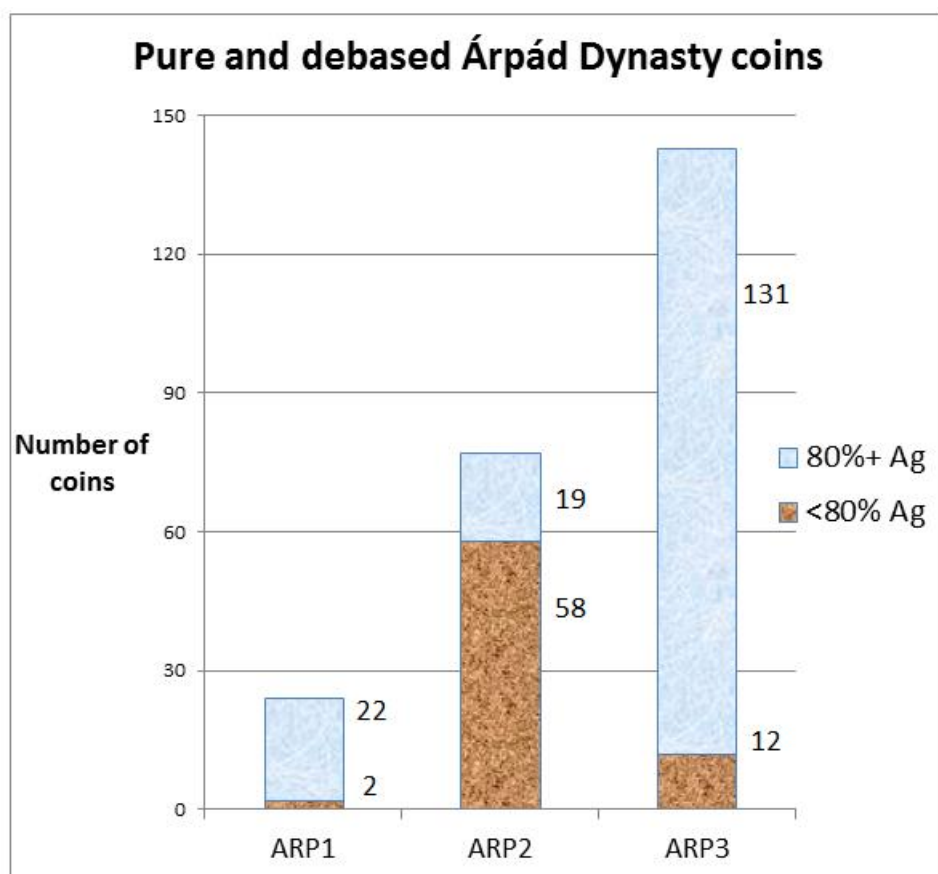


Figure 6

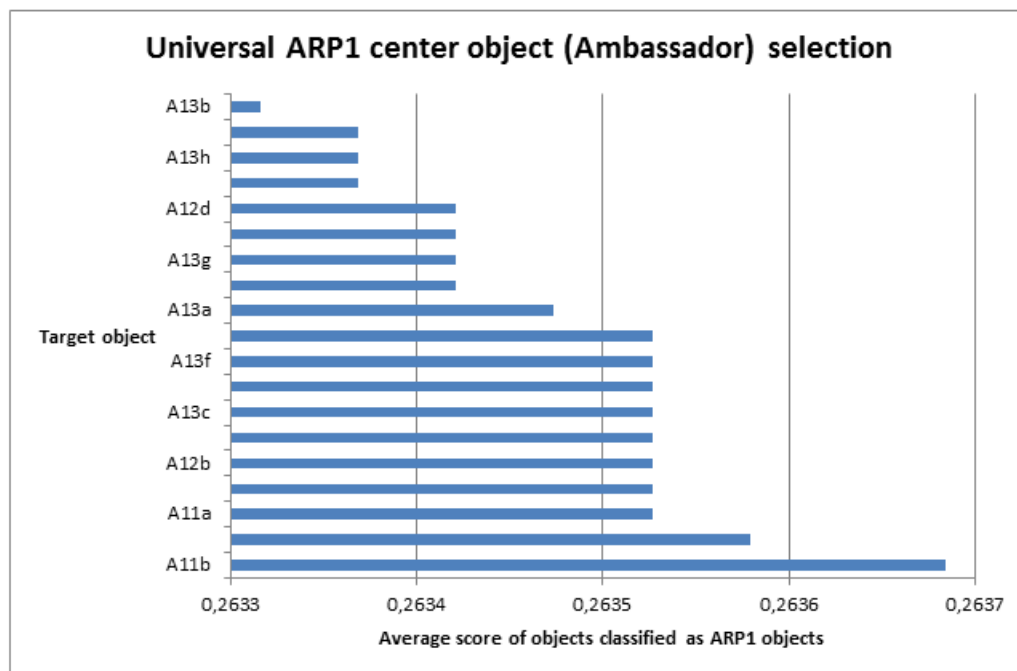


Figure 7.

